Active Control of a Nonlinear Flexible Aircraft Wing

Jiffri, S.[a], Mottershead, J.E.[a], Cooper, J.E.[b]

[a] *Centre for Engineering Dynamics, School of Engineering, The University of Liverpool, Brownlow Hill, Liverpool L69 3GH.*
[b] *Department of Aerospace Engineering, University of Bristol, Queens Building, University Walk, Bristol BS8 1TR.*

SUMMARY: The avoidance of flutter still remains a key constraint in the design of all aircraft. In this endeavour, the need to develop models that accurately reproduce physical phenomena is of growing importance; one such phenomenon is nonlinearity. Whereas in many cases it may be justifiable to neglect nonlinearity and treat the system as linear, substantial nonlinear behaviour (such as limit cycle oscillations) have been observed in several aircraft, making evident the need to account for nonlinearity. The present work gains motivation from this need.

In the first section, the Feedback Linearisation method is applied to a structurally nonlinear flexible aircraft wing, and Active Control is performed to extend the flutter boundary of the system. The flexible wing is modelled as an aeroservoelastic system containing ailerons that will provide the required control forces. The ailerons are treated purely as an excitation source, and do not participate in the dynamics of the system. In the second section, some uncertainty is incorporated into the parameters describing the nonlinearity, and Adaptive Feedback Linearisation is performed to account for this uncertainty. The advantage of this method is the guaranteed closed-loop stability of the system, despite a lack of knowledge of the exact description of the nonlinearity. Results from numerical simulations demonstrate the effectiveness of the method in suppressing flutter.

KEYWORDS: flutter, aeroelasticity, aeroservoelasticity, nonlinearity, feedback linearisation, adaptive feedback linearisation, control

1. INTRODUCTION

The suitability of linear control methods to a given system is clearly dependent on the extent of nonlinearities likely to be present in the system. In weakly nonlinear regimes, the system may be assumed linear. However if there are clear indications of substantial nonlinearity, it becomes necessary to apply a more rigorous approach, in the interests of achieving effective control. Some significant effects arising from system nonlinearities in aeroelastic systems are documented in [1, 2]. The present work considers a situation where limit cycle oscillation (LCO) in nonlinear response is caused by a structural nonlinearity.

Application of linear control methods on a nonlinear system with hardening stiffness was investigated experimentally by Block and Strganac in [3]. It is found that the effectiveness of linear control is limited to situations where the airspeed is not much higher than the linear flutter speed, where the LCO amplitude is small. For airspeeds substantially higher than the linear flutter speed (where LCO amplitudes are higher) the control becomes unpredictable, and its effectiveness limited.

Ko et al. apply Feedback Linearisation to a 2-DOF rigid aeroelastic system with torsional nonlinearity [4]. It is shown that using a single control surface leads to local stability, whereas global stability may be achieved using two control surfaces. This work is extended in [5], where the same authors perform a detailed analysis of plunge mode control, and also introduce adaptive feedback linearisation in the two control surface case to account for nonlinearity parameter errors. The latter is implemented experimentally by Platanitis and Strganac [6], with results indicating an improvement when using an additional control surface, but only up to moderately high air velocities. A later publication by Ko et al. [7] examines the case where only a single control surface is employed. In this case, global stability is only guaranteed if the zero-dynamics of the uncontrolled sub-system is stable.

The Adaptive control method was later implemented experimentally by Strganac et al. [8], with results suggesting that knowledge of the exact nonlinearity parameters is critical to the performance of feedback linearisation in the absence of adaptive methods, and that the adaptive controller substantially improves the controlled response. It is also observed in [8] that performing feedback linearisation without adaptation in the presence of parameter errors can cause the system to reach non-zero equilibria, rather than the zero equilibrium that is usually sought.

Monahemi and Kristic employ adaptive feedback linearisation to suppress wing-rock motion, a phenomenon triggered primarily by aerodynamic nonlinearities [9]. In their work, the role of adaptive control was to update the aerodynamic parameters. Other applications of adaptive feedback linearisation include work by Fossen and Paulsen on the automatic steering of ships [10]. Among other related work is [11], where the authors design a control law based on a backstepping design technique to control a nonlinear aeroelastic system whose parameters are assumed unknown, based on Output feedback. Successful control of pitch and plunge motions is demonstrated through simulations. A further advantage of this method is that it does not require high-gain feedback, which may lead to control saturation and potentially destabilise the system.

In this paper, Adaptive Feedback Linearisation is applied to a flexible wing with a structural nonlinearity. The latter is introduced to the system by coupling a rigid pylon-engine to the wing via a nonlinear hardening torsional spring. An uncertainty in the parameter describing the nonlinearity is introduced, and the controlled response compared when adaptive feedback linearisation and exact feedback linearisation are applied. Specifically, the use of 2 inputs and 2 outputs to control the 3-DOF system is considered, and the role of the resulting internal dynamics investigated.

2. THE AEROSERVOELASTIC MODEL

The governing equation of the aeroservoelastic model takes the usual form given by

$$\mathbf{A}\ddot{\mathbf{q}} + \left(\rho V \mathbf{B} + \mathbf{D}\right)\dot{\mathbf{q}} + \left(\rho V^2 \mathbf{C} + \mathbf{E}\right)\mathbf{q} = \mathbf{f}\,, \tag{1}$$

where $\mathbf{A}, \mathbf{D}, \mathbf{E}$ are the inertia, structural damping and structural stiffness matrices respectively, $\mathbf{B}, \mathbf{C}$ are the aerodynamic damping and aerodynamic stiffness matrices respectively, and ρ, V are air density and velocity respectively. The vector $\mathbf{q}$ contains generalised co-ordinates describing the motion of the system, whereas the vector $\mathbf{f}$ contains externally applied generalised forcing terms.

In this work, modified aerodynamic strip theory has been used to compute the lift and pitch moment acting on the wing. An additional unsteady aerodynamic derivative term is included to account for significant unsteady effects.

Following an assumed-mode-shapes approach [12, 13], the flexible wing has been assumed to consist of two deflection patterns, namely the first flexural (bending) mode, and first torsional mode. These shapes are depicted in Figure 1 along with the co-ordinate system used (the origin is at the Leading Edge, root of the wing).

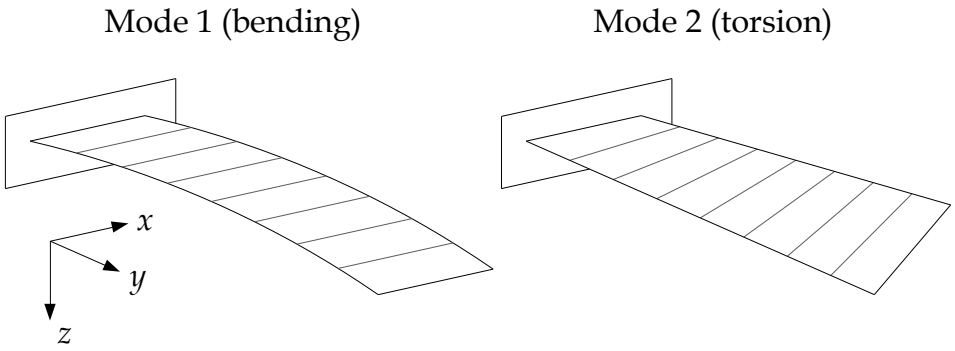

Figure 1 – The two deflection patterns assumed for the flexible wing

Thus, the wing comprises two degrees of freedom (DOFs). The assumed shapes are incorporated into the wing model by specifying the vertical deflection of the wing z at any point (x, y) in terms of contributions from all deflection patterns, viz.,

$$z = y^2 q_1 + y\left(x - x_f\right) q_2 \,, \tag{2}$$

where q_1, q_2 are generalised co-ordinates that quantify the amount of bending and torsion modes present in the overall deflection. The angle of twist at a given distance *y* is given by

$$\theta_{wt} = y q_2 \,, \tag{3}$$

where the subscript "*wt*" denotes wing twist. A third generalised co-ordinate q_{pe} pertains to the motion of the pylon-engine (signified by the subscript "*pe*"). The pylon-engine has been modelled as a rigid body, consisting of a solid cylinder (engine) onto which a thin parallelogram-shaped plate (pylon) has been fixed at the top. This rigid assembly is depicted in Figure 2 below:

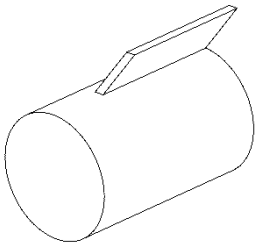

Figure 2 - 3D view of pylon-engine

For the purpose of this model, in order to restrict the overall dimension of the model to a value that may be easily accommodated by the Feedback Linearisation process, the pylon-engine is modelled with only 1 DOF (this brings the dimension of the coupled wing-pylon-engine model to three). Specifically, this is a rotation of the pylon-engine about an axis that is parallel to the global *y*-axis, going through the attachment point to the wing (this axis will be referred to as a local *y*-axis). A sketch of the combined wing-pylon-engine is shown in Figure 3.

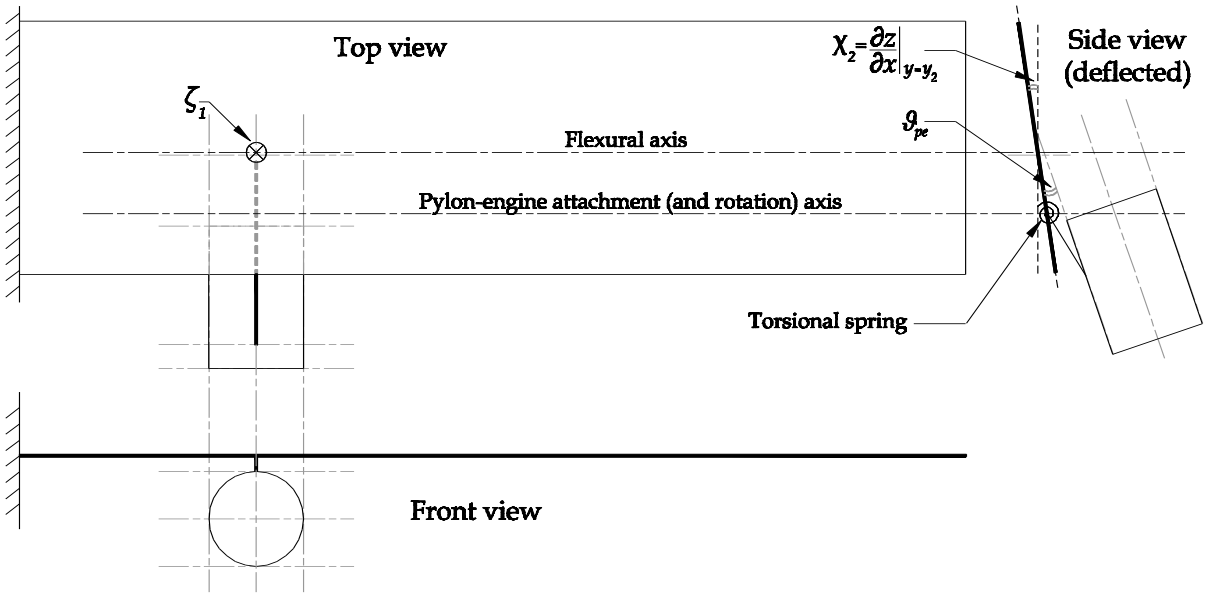

Figure 3 - Various views of the wing- pylon-engine model
(pylon represented by a rigid link, in side view)

Note that the pylon-engine rotational DOF ϑ_{pe} is the deflection of the pylon-engine *relative* to the wing. The absolute rotation θ_{pe}, may be obtained by adding the wing twist angle at the engine attachment location, χ_2, to ϑ_{pe}.

2.1. Co-ordinate Transformation

Since the wing deflection has been defined in assumed-mode-shapes generalised co-ordinates, in order to couple the pylon-engine, it is necessary to represent the latter also in the assumed-modes space. This may be achieved by a co-ordinate transformation. In order to ensure that the transformation is an equivalence transformation – such that it is possible to transform back and forth between the assumed-modes and physical domains – it is necessary to specify a number of physical co-ordinates that is equal to the number of assumed modes in the system, in the present case, three. One has already been chosen as ϑ_{pe}. The remaining two are chosen as:

a) A vertical deflection at point 1, which lies at the crossing between the wing flexural axis and the local *x*- axis going through the attachment point of the pylon-engine to the wing. This co-ordinate is named as ζ_1.

b) The wing twist angle at point 2, the pylon-engine attachment location, which is chosen as the intersection of the quarter-semi-span and quarter-chord. This co-ordinate is named as χ_2.

The particular choice of the above two co-ordinates is due to the requirement of these co-ordinates in the derivation of the system equations. Figure 3 above depicts the three physical co-ordinates on the wing-pylon-engine system. Thus, the required transformation takes the form

$$\mathbf{z} = \mathbf{T}\mathbf{q}, \quad \text{where } \mathbf{z} = \begin{Bmatrix} \zeta_1 & \chi_2 & \vartheta_{pe} \end{Bmatrix}^T, \quad \mathbf{q} = \begin{Bmatrix} q_1 & q_2 & q_{pe} \end{Bmatrix}^T, \tag{4}$$

and $\mathbf{T}$ is the equivalence transformation matrix. Using equation (2), and defining $\theta_{pe} = \varsigma q_{pe}$, where ς is some arbitrary scalar multiple (this value may be set to 1, which results in the absolute pylon-engine rotation in the physical and assumed-modes domains being identical), $\mathbf{T}$ may be derived as

$$\mathbf{T} = \begin{bmatrix} y_1^2 & 0 & 0 \\ 0 & y_2 & 0 \\ 0 & -y_2 & \varsigma \end{bmatrix}, \tag{5}$$

where y_1, y_2 are the *y*- co-ordinates at points 1 and 2 respectively. Using the Lagrange equation and aerodynamic strip theory [13], assuming the same ordering of co-ordinates as in the above equation, the system matrices of the wing and pylon-engine in the assumed-modes domain may be derived separately. For the bending and torsion modes of the wing,

$$\mathbf{A}_{w,mod} = m \begin{bmatrix} \frac{s^5 c}{5} & \frac{s^4}{4}\left(\frac{c^2}{2} - c x_f\right) & 0 \\ \frac{s^4}{4}\left(\frac{c^2}{2} - c x_f\right) & \frac{s^3}{3}\left(\frac{c^3}{3} - c^2 x_f + c x_f^2\right) & 0 \\ 0 & 0 & 0 \end{bmatrix}, \quad \mathbf{E}_{w,mod} = \begin{bmatrix} 4EIs & 0 & 0 \\ 0 & GJs & 0 \\ 0 & 0 & 0 \end{bmatrix}, \tag{6}$$

where c, s are the wing chord and semi-span respectively, m the wing mass per unit area, x_f the *x*-co-ordinate of the flexural axis, EI, GJ the wing flexural and torsional rigidity respectively. For the pylon-engine motion,

$$\mathbf{A}_{pe,mod} = \begin{bmatrix} m_{pe} y_1^4 & 0 & m_{pe} y_1^2 r_G \hat{c} \varsigma \\ 0 & 0 & 0 \\ m_{pe} y_1^2 r_G \hat{c} \varsigma & 0 & \left(I_G + m_{pe} r_G^2\right)\varsigma^2 \end{bmatrix}, \quad \mathbf{E}_{pe,mod} = K_T \begin{bmatrix} 0 & 0 & 0 \\ 0 & y_2^2 & -y_2 \varsigma \\ 0 & -y_2 \varsigma & \varsigma^2 \end{bmatrix}, \tag{7}$$

where m_{pe} is the combined mass of the pylon and engine, I_G the moment of inertia of the pylon-engine referred to a local *y*- axis going through the pylon-engine centre of mass (COM), $\hat{c}$ the cosine of the angle of the pylon-engine COM relative to the top flat surface of the pylon taken about the flexural axis, r_G the distance between the flexural axis and the local *y*- axis mentioned above, and K_T the linear torsional coupling stiffness. The aerodynamic damping and aerodynamic stiffness matrices, respectively, are given by

$$\mathbf{B}_{mod} = \begin{bmatrix} \frac{c\,a_W s^5}{10} & 0 & 0 \\ -\frac{c^2 e a_W s^4}{8} & -\frac{c^3 s^3 M_{\dot{\theta}}}{24} & 0 \\ 0 & 0 & 0 \end{bmatrix}, \quad \mathbf{C}_{mod} = \begin{bmatrix} 0 & \frac{cs^4 a_W}{8} & 0 \\ 0 & -\frac{ec^2 s^3 a_W}{6} & 0 \\ 0 & 0 & 0 \end{bmatrix}, \tag{8}$$

where e, the eccentricity ratio, is distance between the aerodynamic centre and flexural axis as a fraction of the chord, a_W the lift curve slope and $M_{\dot{\theta}}$ the non-dimensional pitch damping derivative. The overall inertial and structural stiffness matrices are obtained by summing the wing and pylon-engine components, viz.,

$$\mathbf{A}_{mod} = \mathbf{A}_{w,mod} + \mathbf{A}_{pe,mod}\,, \qquad \mathbf{E}_{mod} = \mathbf{E}_{w,mod} + \mathbf{E}_{pe,mod}\,. \tag{9}$$

An appropriate level of structural damping $\mathbf{D}_{mod}$ may be included in the model. A convenient way of doing this is to specify the damping in the normal-modes domain as modal damping values, and subsequently transforming into the assumed-modes domain using the eigenvectors of the undamped system.

2.2. Forcing Terms

The aileron (control surface) usually provides the necessary means to apply control forces to the wing-pylon-engine system. It is assumed in this work that two control surfaces are available, the first (closest to the wing root) spanning 85% of the length of the wing and the second spanning the remaining length (the contribution of the control surfaces to the dynamics of the overall system is neglected). The widths of the first and second control surfaces are assumed to be 20% and 33.33% of the chord length respectively. These particular dimensions have been chosen so as to optimise the distribution of work performed by each control surface. Again, using the Lagrange equation and aerodynamic strip theory, the forcing vector is found as

$$\mathbf{f}_{mod} = \tilde{r} \begin{bmatrix} -\frac{4913}{48000} a_{C,1} s & -\frac{3087}{48000} a_{C,2} s \\ \frac{289}{1600} c b_{C,1} & \frac{111}{1600} c b_{C,2} \\ 0 & 0 \end{bmatrix} \begin{Bmatrix} \beta_1 \\ \beta_2 \end{Bmatrix} =: \bar{\mathbf{B}}_{mod} \mathbf{u}\,, \quad \text{where } \tilde{r} = \rho V^2 c s^2\,, \tag{10}$$

and where each surface will have its own deflection angle β_1, β_2 and set of aerodynamic parameters a_C, b_C [14].

2.3. Inclusion of Nonlinearity

Nonlinearity may be incorporated by adding an internal force to the overall equation of motion, viz.,

$$\mathbf{A}_{mod}\ddot{\mathbf{q}} + \left(\rho V \mathbf{B}_{mod} + \mathbf{D}_{mod}\right)\dot{\mathbf{q}} + \left(\rho V^2 \mathbf{C}_{mod} + \mathbf{E}_{mod}\right)\mathbf{q} + \mathbf{f}_{nl,mod} = \mathbf{f}_{mod}\,. \tag{11}$$

For the purpose of the present model, a cubic hardening nonlinearity is assumed in the torsional spring connecting the pylon-engine to the wing. The nonlinear force developed in the spring may be expressed as

$$f_{T,nl} = K_{T,nl} \vartheta_{pe}^3\,, \tag{12}$$

where $K_{T,nl}$ is the stiffness coefficient of the cubic nonlinearity. As this nonlinear force occurs within the system, an equal and opposite force will arise in the coupled DOF. Since ϑ_{pe} is a relative deflection (involving both the coupling DOFs), the overall nonlinear force vector will take the form

$$\mathbf{f}_{nl,mod} = \mathbf{T}^T \mathbf{f}_{nl}\,, \quad \text{where } \mathbf{f}_{nl} = \begin{Bmatrix} 0 & 0 & f_{T,nl} \end{Bmatrix}^T\,, \tag{13}$$

where the transformation $\mathbf{T}$ is defined in equation (5).

3. NUMERICAL SIMULATION – UNCONTROLLED SYSTEM

A numerical simulation of the 3-DOF aeroservoelastic model is now performed. Initially, appropriate dimensions and parameters for the wing and pylon-engine are chosen. A frequency domain computation is then performed, and thereby the flutter speed is determined. Subsequently, a cubic hardening stiffness is included in the torsional spring connecting the wing to the pylon-engine, and the nonlinear time-domain response is simulated. In these simulations it is assumed that there will be no external excitation.

3.1. Model Dimensions and Parameters

The dimensions and parameters chosen for the model are given in Table 1 and Table 2.

Table 1 – Dimensions and Parameters of Flexible Wing

Semi-span (s)	7.5 m	Flexural rigidity (EI)	3,675 kNm^2	Eccentricity ratio (e)	0.23
Chord (c)	2.0 m	Torsional rigidity (GJ)	1,890 kNm^2		
Flexural axis (x_f)	0.96 m	Air density (ρ)	1.225 kgm^{-3}	Non-dimensional pitch damping derivative ($M_{\dot{\theta}}$)	-1.2
Mass/unit area (m)	100 kgm^{-2}	Lift curve slope (a_W)	2π		

Table 2 – Dimensions and Parameters of Pylon-Engine

Engine diameter (d_e)	0.75 m	Engine mass (m_e)	350 kg	Engine length (l_e)	1.125 m
Pylon mass (m_p)		35 kg	Pylon height (h_p)		0.125 m
Coupling torsional spring stiffness (K_T)		511 kNm/rad	Coefficient of cubic component of coupling stiffness ($K_{T,nl}$)		$300 \times K_T$

A small amount of structural damping is also included in the system. The damping is generated in the normal-modal space, by assigning modal damping of 1% to all modes.

3.2. Airspeed vs. Natural Frequency and Airspeed vs. Damping Ratio Plots

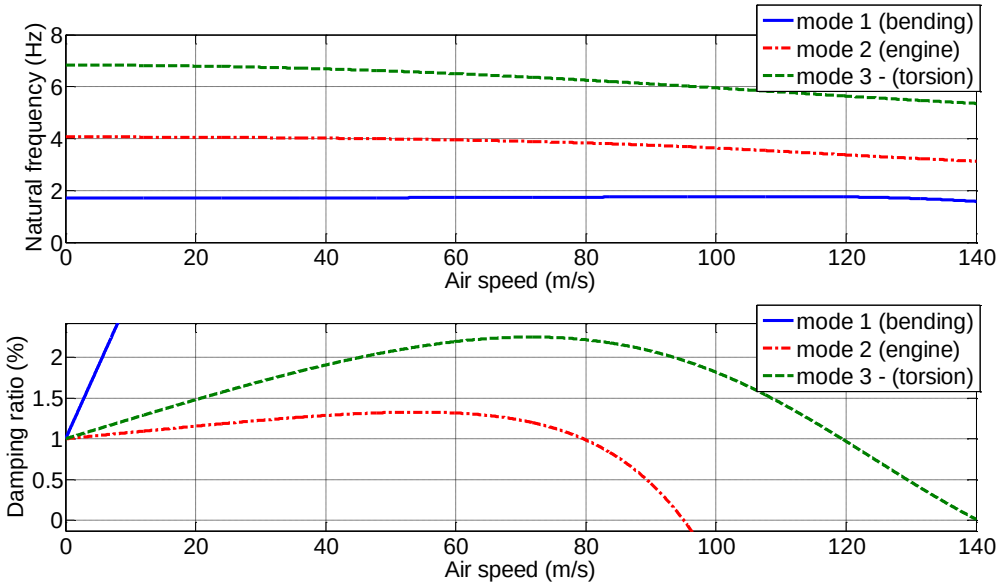

Figure 4 – V-omega and V-zeta plots for the wing-pylon-engine model

The structural modes in the combined model occur at 1.71 Hz (bending), 4.06 Hz (pylon-engine mode) and 6.83 Hz (torsional). It is evident that there are two flutter points, which is a result of coupling the pylon-engine to the wing. The initial flutter occurs at 95.05 ms^{-1} (pylon-engine mode).

3.3. Nonlinear Time-domain Response

The nonlinear system is simulated at an airspeed of 97.5 ms^{-1}, just above the first flutter point, under the application of the initial conditions ζ_1 = 0.333 mm, χ_2 = 0.00333 rad, ϑ_{pe} = 0.05 rad. The resulting response of the system clearly exhibits LCO. A sample of the response for the q_2 co-ordinate is shown in Figure 5.

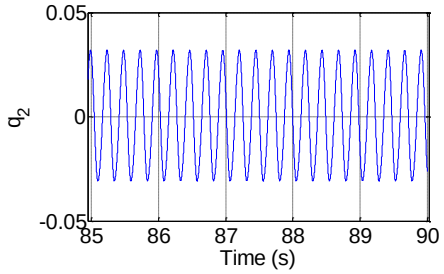

Figure 5 – Zoomed in plot of uncontrolled q_2 response, showing LCO

4. LINEARISED CLOSED-LOOP SYSTEM USING NONLINEAR CONTROL

Feedback Linearisation [15] is a process applied to a nonlinear system to essentially transform it into a linear system. Unlike Jacobian Linearisation, it is exact, and does not entail an approximation at any stage. The method is implemented by transforming the nonlinear system given by

$$\dot{\mathbf{x}} = \mathbf{f}(\mathbf{x}) + \mathbf{G}(\mathbf{x})\mathbf{u} \tag{14}$$

into an equivalent linear system

$$\mathbf{z} = \underline{\mathbf{A}}\mathbf{z} + \underline{\mathbf{B}}\bar{\mathbf{u}}\,, \tag{15}$$

based on a particular choice of output $\mathbf{y} = \mathbf{h}(\mathbf{x})$. In the above equations $\mathbf{u}$ and $\bar{\mathbf{u}}$ are the inputs to the nonlinear and linearised systems respectively, which are often referred to as the actual and artificial inputs respectively. The mapping from the nonlinear domain to the linearised domain is achieved through a non-singular co-ordinate transformation $\mathbf{z} = \underline{\mathbf{T}}(\mathbf{x})$, which is nonlinear. In addition, a mapping between $\mathbf{u}$ and $\bar{\mathbf{u}}$ is also required

In the present case, as the number of inputs and outputs is less than the dimension of the overall model, only a partial linearisation of the system may be achieved. The portion of the system that remains untransformed will contribute to what is known as the *internal dynamics* of the system, whose stability must be ensured for stability of the overall closed-loop system. The latter is achieved by examining the stability of the zero-dynamics [15], which is obtained by setting all co-ordinates pertaining to the linearised sub-system to zero in the expressions for the internal dynamics. The zero-dynamics may be either linear or nonlinear. It is pointed out that since the zero-dynamics does not contain input terms, it is uncontrollable.

Feedback Linearisation is now applied to the nonlinear model developed above. For the task at hand, it is more appropriate to use the assumed-modes representation of the system matrices. This is because once the system has been linearised, pole-placement may be performed directly on the assumed modes to shift their respective poles to more desirable locations, or simply stabilise the system.

4.1. Nonlinear State-Space Model

The nonlinear model in equation (11) may be expressed in the following state-space form:

$$\dot{\mathbf{x}} = \mathbf{f}(\mathbf{x}) + \mathbf{G}(\mathbf{x})\mathbf{u}\,, \quad \text{with } \mathbf{x} =: \begin{Bmatrix} x_1 & x_2 & x_3 & x_4 & x_5 & x_6 \end{Bmatrix}^T, \tag{16}$$

where $\mathbf{u} = \{\beta_1 \quad \beta_2\}^T$ is the vector of actual inputs, as defined in section 2.2 above. The outputs are chosen as

$$\mathbf{y} = \{y_a \quad y_b\}^T := \{q_1 \quad q_2\}^T = \{x_1 \quad x_2\}^T . \tag{17}$$

Now, following the procedure of Input-Output Feedback Linearisation [15], the outputs are differentiated with respect to time, whilst substituting from equation (16) at each stage. This results in

$$\begin{aligned} \dot{y}_a &= x_4 , & \dot{y}_b &= x_5 , \\ \ddot{y}_a &= f_4 + \begin{bmatrix} g_{41} & g_{42} \end{bmatrix} \mathbf{u} , & \ddot{y}_b &= f_5 + \begin{bmatrix} g_{51} & g_{52} \end{bmatrix} \mathbf{u} , \end{aligned} \tag{18}$$

where f_i denotes the i^{th} term of the vector $\mathbf{f}(\mathbf{x})$, and g_{ij} denotes the ij^{th} term of the matrix $\mathbf{G}(\mathbf{x})$. The Relative Degree of the system for the particular choice of outputs, may now be computed. Since the present system has multiple inputs and multiple outputs, each output will have an associated Relative Degree. Thus, the Relative Degree of the overall system will consist of all these values, and may be cast as a vector. For the present system, the Relative Degree will be $\{2 \quad 2\}^T$, provided that the matrix

$$\begin{bmatrix} g_{41} & g_{42} \\ g_{51} & g_{52} \end{bmatrix} =: \boldsymbol{\Xi} \tag{19}$$

is non-singular for all $\mathbf{x}$. In this particular case, since the above matrix does not depend on $\mathbf{x}$, provided that it is non-singular, the computed value of Relative Degree will be globally valid.

4.2. Linearising Feedback

A new co-ordinate system is now defined, which will provide a mapping from the equivalent linear system that is sought, to the original nonlinear system. The co-ordinates corresponding to the linearised sub-system are defined as

$$\begin{aligned} z_1 &:= y_a = q_1 = x_1 , & z_2 &:= \dot{y}_a = \dot{q}_1 = \dot{x}_1 = x_4 , \\ z_3 &:= y_b = q_2 = x_2 , & z_4 &:= \dot{y}_b = \dot{q}_2 = \dot{x}_2 = x_5 . \end{aligned} \tag{20}$$

Using the above expressions in conjunction with appropriate expressions that describe the normal form of the internal dynamics, it can be shown that the required co-ordinate transformation is

$$\begin{Bmatrix} z_1 \\ z_2 \\ z_3 \\ z_4 \\ z_5 \\ z_6 \end{Bmatrix} = \begin{bmatrix} 1 & 0 & 0 & 0 & 0 & 0 \\ 0 & 0 & 0 & 1 & 0 & 0 \\ 0 & 1 & 0 & 0 & 0 & 0 \\ 0 & 0 & 0 & 0 & 1 & 0 \\ 0 & 0 & 1 & 0 & 0 & 0 \\ 0 & 0 & 0 & \bar{\xi}_1 & \bar{\xi}_2 & \bar{\xi}_3 \end{bmatrix} \begin{Bmatrix} x_1 \\ x_2 \\ x_3 \\ x_4 \\ x_5 \\ x_6 \end{Bmatrix} , \tag{21}$$

where

$$\bar{\xi}_1 = \left(g_{51} g_{62} - g_{61} g_{52} \right) , \quad \bar{\xi}_2 = \left(g_{61} g_{42} - g_{41} g_{62} \right) , \quad \bar{\xi}_3 = \left(g_{41} g_{52} - g_{51} g_{42} \right) . \tag{22}$$

Note that this non-singular transformation is independent of $\mathbf{x}$, and is therefore globally valid. Now, choosing the vector of actual inputs so as to cancel the nonlinearity in the controlled subsystem, it may be shown that the state-space equations $\dot{\mathbf{z}} = \underline{\mathbf{A}}\mathbf{z} + \underline{\mathbf{B}}\bar{\mathbf{u}}$ decouple to provide the following two controlled single-DOF systems:

$$\begin{Bmatrix} \dot{z}_1 \\ \dot{z}_2 \end{Bmatrix} = \begin{bmatrix} 0 & 1 \\ 0 & 0 \end{bmatrix} \begin{Bmatrix} z_1 \\ z_2 \end{Bmatrix} + \begin{bmatrix} 0 \\ 1 \end{bmatrix} \bar{u}_1 , \quad \begin{Bmatrix} \dot{z}_3 \\ \dot{z}_4 \end{Bmatrix} = \begin{bmatrix} 0 & 1 \\ 0 & 0 \end{bmatrix} \begin{Bmatrix} z_3 \\ z_4 \end{Bmatrix} + \begin{bmatrix} 0 \\ 1 \end{bmatrix} \bar{u}_2 . \tag{23}$$

where $\bar{\mathbf{u}} =: \{\bar{u}_1 \quad \bar{u}_2\}^T$ is the vector of (artificial) inputs to the linear system. Note that the above two single-DOF systems correspond to the assumed-modes generalised co-ordinates q_1, q_2 respectively (see equation (20)). The artificial inputs may be chosen as a linear combination of instantaneous displacement and velocity, so as to modify the natural frequency and damping ratio of each of these systems respectively, viz.,

$$\bar{u}_1 = -\begin{bmatrix} \bar{f}_1 & \bar{g}_1 \end{bmatrix} \begin{Bmatrix} z_1 \\ z_2 \end{Bmatrix}, \quad \bar{u}_2 = -\begin{bmatrix} \bar{f}_2 & \bar{g}_2 \end{bmatrix} \begin{Bmatrix} z_3 \\ z_4 \end{Bmatrix}. \tag{24}$$

4.3. Zero-Dynamics

In addition to the two controlled sub-systems in equation (23), a further 2-dimensional system describing the Internal Dynamics will remain. Using the expressions for the latter, the zero-dynamics may be derived as

$$\begin{Bmatrix} \dot{z}_5 \\ \dot{z}_6 \end{Bmatrix}_{ZD} = \begin{bmatrix} 0 & \dfrac{1}{\bar{\xi}_3} \\ \bar{\boldsymbol{\xi}}^T \boldsymbol{\psi}_{(:,3)} & \dfrac{1}{\bar{\xi}_3} \bar{\boldsymbol{\xi}}^T \boldsymbol{\phi}_{(:,3)} \end{bmatrix} \begin{Bmatrix} z_5 \\ z_6 \end{Bmatrix}_{ZD} + \begin{Bmatrix} 0 \\ K_{T,nl} \varsigma^3 \bar{\boldsymbol{\xi}}^T \boldsymbol{\Omega} \begin{Bmatrix} 0 \\ -y_2 \\ \varsigma \end{Bmatrix} z_{5,ZD}^3 \end{Bmatrix}, \tag{25}$$

where $\bar{\boldsymbol{\xi}}^T = \{\bar{\xi}_1 \quad \bar{\xi}_2 \quad \bar{\xi}_3\}^T$. It is evident that the zero-dynamics are nonlinear. However, further investigation reveals that the only possible equilibrium point of the above system is the trivial case [0, 0], and that for non-zero structural damping the linear component of the zero-dynamics will have eigenvalues with negative real parts, thus ensuring that the zero-dynamics and hence the overall closed-loop system is asymptotically stable.

4.4. Adaptive Feedback Linearisation

In situations where there is a discrepancy between the actual nonlinearity and assumed nonlinearity used in the linearising feedback, this parameter discrepancy acts as an input to the closed-loop system. It is conceivable that this additional (unknown) input may potentially destabilise the system, or at least degrade control performance. This possibility may be eliminated by accounting for the nonlinearity errors using an adaptive algorithm. Such an algorithm seeks to guarantee asymptotic stability of closed-loop response.

A scalar Lyapunov function V involving $\mathbf{z}_{lin}, \tilde{K}_{T,nl}$ may be defined, such that asymptotic stability of the closed-loop system is guaranteed by ensuring that $V > 0$ and its time-derivative $\dot{V} < 0$ [16]. Here, $\mathbf{z}_{lin} = \mathbf{z}_{(1:4)}$ and $\tilde{K}_{T,nl}$ is the nonlinearity parameter error. Such a function may be used as a basis for computing a parameter update law. This approach is valid provided that the zero-dynamics are asymptotically stable, which in the present case it is. The control law

$$V\left(\mathbf{z}_{lin}, \tilde{K}_{T,nl}\right) = \mathbf{z}_{lin}^T \mathbf{P} \mathbf{z}_{lin} + \tilde{K}_{T,nl}^2, \tag{26}$$

is considered, where $\mathbf{P}$ is a positive definite, symmetric matrix. Using the above expression, in conjunction with another expression that quantifies the additional input to the close-loop system, it is possible to derive an expression for the parameter update law as

$$\dot{\tilde{K}}_{T,nl} = -\vartheta_{pe}^3 \mathbf{s}^T \boldsymbol{\Omega}_{([1\,2],:)}^T \underline{\mathbf{B}}_{lin}^T \mathbf{P} \mathbf{z}_{lin}, \tag{27}$$

where

$$\mathbf{s} = \{0 \quad -y_2 \quad \varsigma\}^T, \quad \boldsymbol{\Omega} = -\mathbf{A}_{mod}^{-1}, \quad \underline{\mathbf{B}}_{lin} = \begin{bmatrix} 1 & 0 & 0 & 0 \\ 0 & 0 & 1 & 0 \end{bmatrix}^T, \tag{28}$$

and $\mathbf{P}$ is chosen such that

$$\mathbf{Q} = -\left(\underline{\mathbf{A}}_{cl,lin}^{T}\mathbf{P} + \mathbf{P}\underline{\mathbf{A}}_{cl,lin}\right), \tag{29}$$

where $\mathbf{Q}$ is an arbitrary, positive definite matrix, and

$$\underline{\mathbf{A}}_{cl,lin} = \begin{bmatrix} 0 & 1 & 0 & 0 \\ -\bar{f}_1 & -\bar{g}_1 & 0 & 0 \\ 0 & 0 & 0 & 1 \\ 0 & 0 & -\bar{f}_2 & -\bar{g}_2 \end{bmatrix}. \tag{30}$$

In the present case, since $\underline{\mathbf{A}}_{cl,lin}$ consists of two decoupled 2×2 block-diagonal matrices, if $\mathbf{Q}$ is chosen such that its off-diagonal terms are zero (e.g. a positive multiple of the identity matrix), $\mathbf{P}$ will also have the same structure as $\underline{\mathbf{A}}_{cl,lin}$. Thus, the task of finding $\mathbf{P}$ may be simplified by computing each 2×2 block at a time, and then arranging them along a block-diagonal to form $\mathbf{P}$.

5. NUMERICAL SIMULATION – CLOSED LOOP SYSTEM

Closed-loop control is applied to the nonlinear model in the assumed-modes domain to provide linearising feedback. The latter is computed such that the linearised system consists of the uncoupled SDOF sub-systems referred to in the above section. Initially, it is assumed that no uncertainty in the nonlinearity parameter exists, and on this basis the following modal parameters are set for the pole-placement of the system:

q_1	0.93 Hz	0.01	q_2	4.95 Hz	0.01

In this situation, as one would expect, the two controlled assumed-modes are modified such that their natural frequencies and damping ratios are identical to those in the above table, as seen in Figure 6.

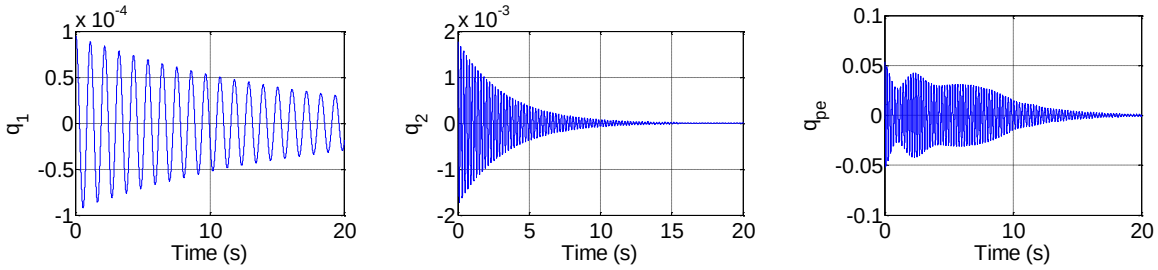

Figure 6 – Feedback-linearised response at 97.5 ms^{-1} (assumed-modes co-ordinates)

It is also evident from the above figure that the remaining co-ordinate, q_{pe}, eventually stabilises because the zero-dynamics of the system are stable. However, when a 40% error in $K_{T,nl}$ is incorporated, and the closed-loop response is simulated based on the above feedback parameters, a degradation in performance is observed, as seen in Figure 7.

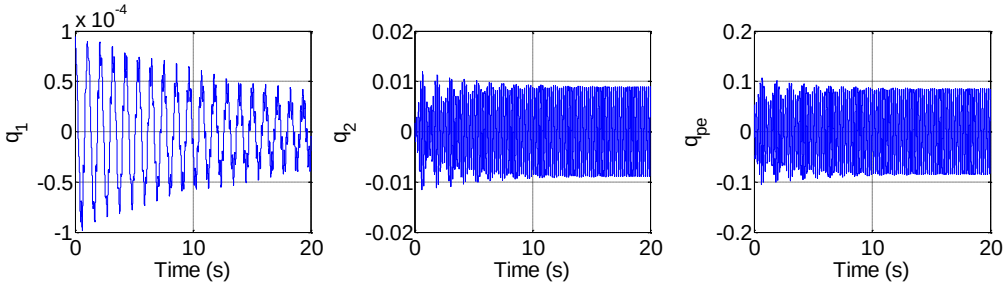

Figure 7 – Feedback-linearised response at 97.5 ms^{-1}, with nonlinearity parameter error included

It is evident that the control fails to eliminate the LCO and fully stabilise the system (running the simulation for a longer duration confirms this observation). This may be resolved by implementing the adaptive controller described in section 4.4 above. The closed-loop response obtained by performing adaptive feedback linearisation is shown in Figure 8 below, which is shown for a 60 second duration.

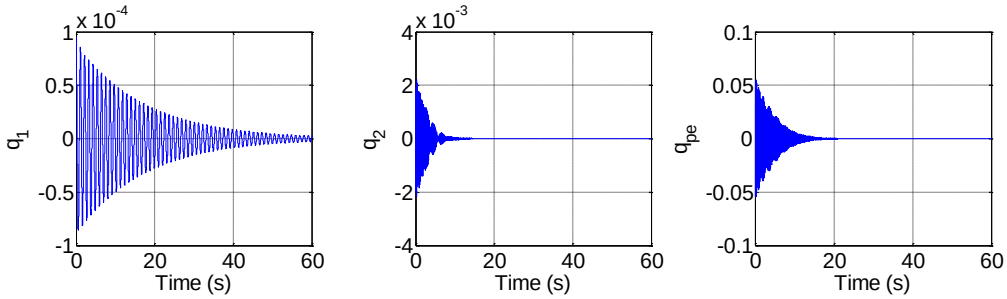

Figure 8 – Feedback-linearised response at 97.5 ms^{-1}, Adaptive Feedback Linearisation

It can also be seen that the controlled responses, as well as the response of the uncontrolled system converge to zero when the adaptive controller is implemented. In fact, this convergence takes place rapidly. When converted to the physical domain, the resulting magnitudes of the co-ordinates occur within acceptable limits ($\zeta_1, \chi_2, \vartheta_{pe}$ take maximum values of 0.33mm, 0.24deg, 2.92deg respectively). It is found that the control surface magnitudes required to achieve the above responses are feasible, as shown in Figure 9.

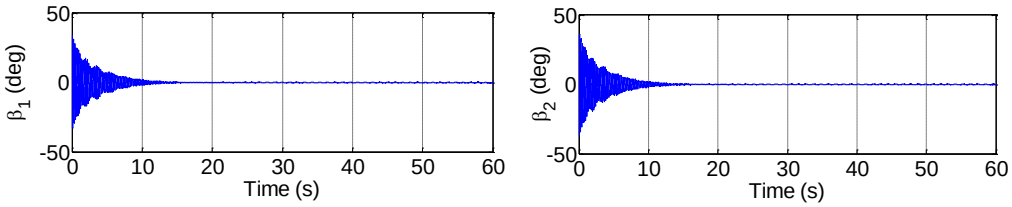

Figure 9 – Inputs required to perform adaptive feedback linearisation, at 97.5 ms^{-1}

6. CONCLUSIONS

Previous work on the application of nonlinear control on aeroelastic systems includes the use of adaptive feedback linearisation in the presence of uncertain system nonlinearities. Much of this work employs a 2-DOF rigid pitch-plunge model. The present work demonstrates the application of adaptive feedback linearisation on a 3-DOF flexible aeroelastic model consisting of a flexible wing and a rigid pylon-engine attached to the wing via a nonlinear torsional spring.

Other work by the present authors addresses the feedback linearisation of the same 3-DOF model using 3 inputs and 3 outputs. In this situation, an advantage is that the entire system is linearised, enabling the control of all 3 co-ordinates of the system. However, a disadvantage is that an actuator capable of controlling the torsional motion of the pylon-engine is required, in addition to the ailerons. Such a device will inevitably give rise to undesirable complexity, in a practical situation. The present work seeks to eliminate the requirement of an additional actuator by considering 2-input 2-output control of the same system. In this case, the system is only partially linearised, and the stability of the internal dynamics is a concern that needs to be addressed.

Simulation results suggest that controlling the wing bending and wing torsional motions using two ailerons located on the wing itself will render the pylon-engine motion uncontrollable. It is seen that the zero-dynamics are nonlinear, but stable in the presence of structural damping. Thus, the conditions for adaptive feedback linearisation are satisfied, and further numerical simulations confirm this fact and reveal that stabilising adaptive control can be implemented with achievable magnitudes of control surface deflection angles. This result is compared with the closed-loop response obtained when one ignores the nonlinearity errors and performs standard feedback linearisation. A marked improvement in response is observed when adaptive control is implemented.

ACKNOWLEDGEMENTS

This research has been funded by EPSRC grant EP/J004987/1 under the project entitled "Nonlinear Active Vibration Suppression in Aeroelasticity".

7. REFERENCES

[1] Dowell E., Edwards J., Strganac T., *Nonlinear aeroelasticity.* Journal of Aircraft, 2003. **40**(5): pp. 857-874.

[2] Lee B.H.K., Price S.J., Wong Y.S., *Nonlinear aeroelastic analysis of airfoils: bifurcation and chaos.* Progress in Aerospace Sciences, 1999. **35**(3): pp. 205-334.

[3] Block J.J., Strganac T.W., *Applied active control for a nonlinear aeroelastic structure.* Journal of Guidance Control and Dynamics, 1998. **21**(6): pp. 838-845.

[4] Ko J., Kurdila A.J., Strganac T.W., *Nonlinear control of a prototypical wing section with torsional nonlinearity.* Journal of Guidance Control and Dynamics, 1997. **20**(6): pp. 1181-1189.

[5] Ko J., Kurdila A.J., Strganac T., *Stability and control of a structurally nonlinear aeroelastic system.* Journal of Guidance Control and Dynamics, 1998. **21**: pp. 718-725.

[6] Platanitis G., Strganac T.W., *Control of a nonlinear wing section using leading- and trailing-edge surfaces.* Journal of Guidance Control and Dynamics, 2004. **27**(1): pp. 52-58.

[7] Ko J., Strganac T.W., Kurdila A.J., *Adaptive Feedback Linearization for the Control of a Typical Wing Section with Structural Nonlinearity.* Nonlinear Dynamics, 1999. **18**(3): pp. 289-301.

[8] Strganac T., Ko J., Thompson D., *Identification and control of limit cycle oscillations in aeroelastic systems.* Journal of Guidance Control and Dynamics, 2000. **23**(6): pp. 1127-1133.

[9] Monahemi M.M., Krstic M., *Control of wing rock motion using adaptive feedback linearization.* Journal of Guidance Control and Dynamics, 1996. **19**(4): pp. 905-912.

[10] Fossen T.I., Paulsen M.J., *Adaptive Feedback Linearization Applied to Steering of Ships.* Modeling, Identification and Control, 1993. **14**(4): pp. 229-237.

[11] Singh S.N., Xing W., *Adaptive Output Feedback Control of a Nonlinear Aeroelastic Structure.* Journal of Guidance Control and Dynamics, 2000. **23**(6): pp. 1109-1116.

[12] Meirovitch L., *Analytical Methods in Vibrations.* 1967: Macmillan USA.

[13] Wright J.R., Cooper J.E., *Introduction to Aircraft Aeroelasticity and Loads*. 2007, Chichester: Wiley.

[14] Fung Y.C., *An Introduction to the Theory of Aeroelasticity*. 1969: Dover.

[15] Isidori A., *Nonlinear Control Systems*. 1995, Berlin Heidelberg New York: Springer.

[16] Atherton D.P., *Stability of Nonlinear Systems*. 1981: John Wiley & Sons Ltd.